Nanopatterned Surface Effect on the Epitaxial growth of InGaN/GaN Multi-quantum Well Light Emitting Diode Structure

Keunjoo Kim*

Department of Mechanical Engineering and Research Center of Industrial Technology, Chonbuk National University, Jeonju 561-756, Republic of Korea

(Received March 6 2009, Accepted April 23 2009)

The authors fabricated a nanopatterned surface on a GaN thin film deposited on a sapphire substrate and used that as an epitaxial wafer on which to grow an InGaN/GaN multi-quantum well structure with metal-organic chemical vapor deposition. The deposited GaN epitaxial surface has a two-dimensional photonic crystal structure with a hexagonal lattice of 230 nm. The grown structure on the nano-surface shows a Raman shift of the transverse optical phonon mode to 569.5 cm^{-1}, which implies a compressive stress of 0.5 GPa. However, the regrown thin film without the nano-surface shows a free standing mode of 567.6 cm^{-1}, implying no stress. The nanohole surface better preserves the strain energy for pseudo-morphic crystal growth than does a flat plane.

Keywords: LED, InGaN/GaN, Multi-quantum well, Nanopatterned surface

1. INTRODUCTION

A great deal of research has been devoted to the development of InGaN/GaN multi-quantum well (MQW) structures into solid-state lighting sources for use in future illumination systems[1-3]. The spontaneous light emission from these materials is very much dependent on the crystalline quality and, especially, on the threading dislocation originating from the lattice mismatch between the GaN and the underlying sapphire substrate. A number of attempts have been made to reduce the dislocation effect using such strategies as the insertion of a microscale epitaxial lateral overgrowth (ELOG) layer of SiO_2 or a SiN_x pattern on the GaN thin film[4,5] as well as the use of microscale patterned sapphire substrate (PSS)[6,7]. The reduction of threading dislocations that results from the hetero-epitaxial interface is attributed to stress localization on the buffer layer preventing the residual stress from propagating into the epitaxial layer. All of these different growth methods are intended to localize the interfacial stress.

In the case of the nanoscale patterns, an SiO_2 nano-rod array ELOG on a GaN layer enhances the photoluminescence (PL) intensity and reduces the dislocation density[8]. By using a porous alumina template, the resulting nanopatterned surface holes enhance light emission and reduce dislocation density[9]. By decreasing the pattern size to nanoscale, the interfacial stress can be reduced[10]. The inclusions of the ELOG and PSS in the epitaxial growth of the InGaN/GaN MQW structure results in an enhanced PL intensity with a reduced dislocation density[11]. It is interesting to clarify how the misfit stress can be transferred from sapphire substrate to the epitaxial layer via the nanopatterned surface.

In this work, we prepared a nanopatterned GaN epitaxial wafer grown on a sapphire substrate in order to regrow the InGaN/GaN MQW LED structure. We characterized the pseudomorphic epitaxial growth at the nanosurface with micro-Raman spectroscopy and photoluminescence measurements.

*Author to whom corresponding should be addressed: electronic mail: kimk@chonbuk.ac.kr

2. EXPERIMENTAL

Figure 1 shows a schematic diagram of the LED structure including the bottom photonic crystal. On a sapphire wafer covered by a GaN buffer layer, we deposited an n-GaN thin film with metal-organic chemical vapor deposition (MOCVD) in the vertical mode of the reactor, then a periodic hole array with a triangular structure was fabricated on this GaN substrate using electron beam nanolithography. On top of this GaN substrate prepared with the nanopatterned area, we grew the InGaN/GaN MQW structure of a blue light-emitting diode (LED) using MOCVD. The nanopattern, which is shown in Fig. 2, was fabricated bye-beam lithography and a subsequent ICP process. The lattice constant was 230 nm, while the diameter and the depth of the holes were 120 and 30 nm, respectively.

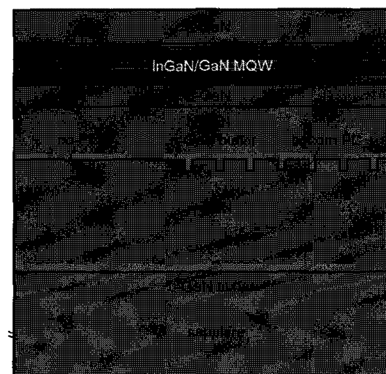

Fig. 1. Schematic diagram of the InGaN/GaN MQW LED structure regrown on nanopatterned surface of n-GaN thin film grown on a sapphire substrate.

 © 2009 KIEEME

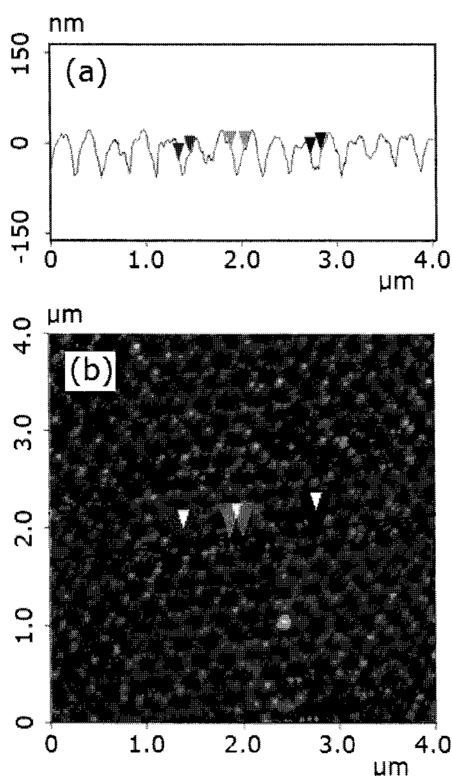

Fig. 2. AFM image of the nanopatterned surface of n-GaN thin film. The nanopattern was processed by e-beam nanolithography with a photonic crystal lattice of 230 nm. The nanoholes have a diameter of 112 nm and a depth of 30 nm.

The full LED structure was constructed on the nanopatterned epitaxial wafer with multiple epitaxial growths of, in order, a 350-Å GaN buffer layer, a Si-doped n-type GaN layer with a thickness of 1 μm, a multi-quantum well (MQW) active layer, and a Mg-doped p-type layer with a thickness of 0.25 μm. The five-period InGaN/GaN MQW structure, which served as the blue LED, had a thickness of 20/100 Å and In compositions of 0.15 for photoluminescence peaks at 430 nm. A rapid thermal annealing process for p-type activation was carried out at a temperature of 550 °C[12]. The Raman and PL spectra were performed in a backscattering geometry using the 514.5-nm and 457.9-nm lines from an Ar^+ ion laser and a 325-nm He-Cd gas laser with power at 100 mW and 30 mW, respectively. The nanostructured surface effect was characterized by a stress analysis derived from the PL and micro-Raman spectra.

3. RESULTS AND DISCUSSION

Figure 3 shows the field emission scanning electron microscope (FE-SEM) images of the surface morphology of the GaN epitaxial thin film. Figure 3(a) shows a square surface 300 μm across that lies in the nanopatterned area. In the boundary region a high density of threading dislocations can be seen, while there is a relatively low density in the central area. The segregated crystalline grains near the edges were grown outside the nanopatterned area.

Figure 3(b) is a magnified image of a point inside the of nanopatterned area shown in Fig. 3(a). The dislocation density is 4.2×10^6 cm^{-2}. The growth-pits of dislocation pinholes are hexagonal in shape with the same orientation as the $(11\underline{2}2)$ facets. This phenomenon is similar to what is seen with a lateral overgrowth on PSS[6], as a growing GaN epilayer on a nanosurface starts to cover the C(0001) plane and nanoholes. The coalesced GaN buffer layer forms nanovoids inside nanoholes.

Figure 3(c) shows the magnified free standing crystalline grains with dimension smaller than ~100 μm that can be seen outside the nanopatterned area in Fig. 3(a). The formation of free standing crystallites indicates that the n-GaN buffer does not provide a 2-dimensional lateral growth condition. GaN homo-epitaxial regrowth on a GaN layer is compressively stressed by a sapphire substrate and a GaN buffer layer without the nanopatterned structure results in a stress relaxation to the substrate-induced misfit strain.

Figure 4 shows the micro-Raman spectra of GaN films regrown on the nanopatterned surface of n-GaN film grown on sapphire substrates. In the nanopatterned area, the Raman intensity is much stronger than in the area without the nanopatterned structure. The spectra show strong E_2(TO)-high modes under $z(x,-)\underline{z}$ scattering geometry. The optical phonon modes of E_2(TO) were observed at 567.6 cm^{-1} from the n-GaN that was regrown on the n-GaN area without a

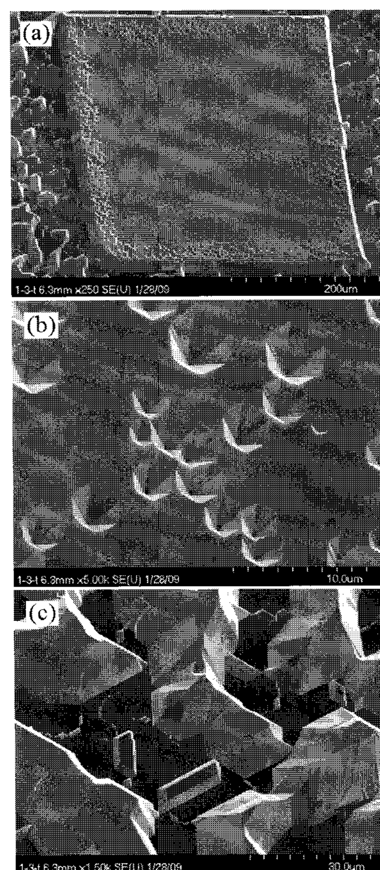

Fig. 3. SEM images of the epitaxially regrown InGaN/GaN MQW LED structure on (a) the nanopatterned surface of n-GaN thin film, (b) an enlarged part of (a), and the regular flat surface without the nanopatterned surface.

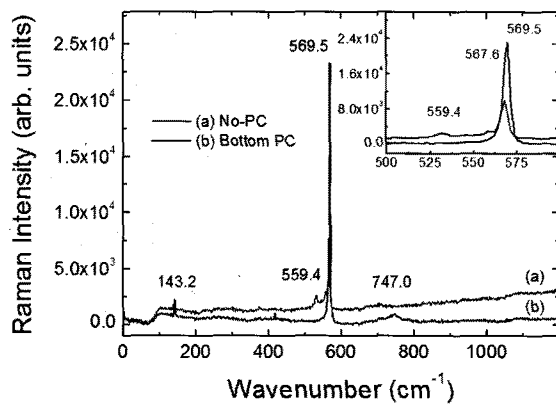

Fig. 4. The Raman spectra of both nanopatterned and regular samples. The regular flat surface provides the home-epitaxial growth for the free standing thin film with the Raman shift of 567.6 cm^{-1}, and the nanopatterned surface shows the value of 569.5 cm^{-1}, indicating that the bottom PC is under the interfacial compressive stress.

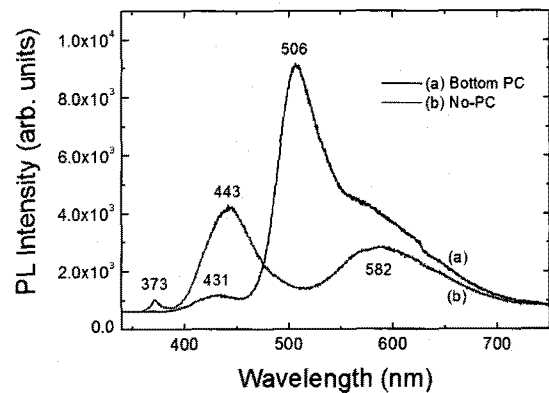

Fig. 5. The PL spectra of nanopatterned and regular samples. The dominant PL peaks at 443 and 506 nm come from the MQWs, and the broad yellow PL band at 582 nm originates from the threading dislocation.

nanopatterned surface and at 569.5 cm^{-1} from the n-GaN that was regrown on the nanopatterned n-GaN surface. From a 400-μm-thick, free-standing, strain-free GaN layer, the E_2(TO) phonon peak was observed at 567.5 cm^{-1}[13,14]. The nanopatterned surface of n-GaN provides the blue shift for the Raman peak, and the corresponding stress can be analyzed in terms of the lattice constant.

Generally, the type of stress is dependent on the substrate; if the substrate is Si(111), there is tensile stress, and there is compressive stress when a sapphire substrate is used. The lattice constants of GaN, Al_2O_3, and Si are 3.189 (5.182), 4.758 (12.991), and 5.43095 Å, respectively. For C(0001) planar growth, the atomic distances of Ga-N, Al-O, and Si-Si are 3.189, 2.747 and 3.840 Å, respectively, indicating that the sapphire (0001) and Si (111) substrates produce compressive and tensile stresses on the GaN epitaxial layer, respectively. Cheong et al.[15] reported that the undoped GaN showed a Raman shift on the E_2(LO) phonon at 568.10 cm^{-1} for the sapphire (0001) substrate, with the phonon peaks of E_g at 576.56 and 751.10 cm^{-1}. Mg-doped p-type GaN showed phonon peaks of 570.39 and 734.60 cm^{-1} for E_2(LO) and A_1(LO) modes, respectively, indicating that p-type doped GaN is more compressive than the undoped GaN. For a 3-μm-diameter, 1.5-μm-thick micro-pyramidal PSS growth, the Raman shift is about 571 cm^{-1}[6]. However, the introduction of a nanoporous structure with a size range of 20-250 nm into a GaN layer grown on a sapphire substrate reduces the Raman shift from 568.4 to 567.7 cm^{-1}, indicating a reduction in compressive stress[16]. Therefore, the nanopatterned surface of n-GaN provides a smaller Raman shift than the micro-patterned surface with a reduced biaxial stress.

For the transparent nanopatterned area, the compressive stress from sapphire substrate can be transferred into the home-epitaxial layers of the regrown and undoped GaN, InGaN/GaN MQW, and p-GaN. However, for the reference area without the nanopattern, the compressive stress originating from the sapphire can be relaxed by the GaN buffer layer, and the nucleation points form a free-standing epitaxial growth of crystallites up to the InGaN/GaN MQW layer and the top p-GaN layer. The Raman shift rate of $\Delta\omega/\omega$ is related to the in-plane lattice strain $\varepsilon=\Delta a/a$, where a is the lattice constant of GaN. The corresponding strain is 3.35×10^{-3}, which originates from the lattice mismatch at the GaN/sapphire interface. For a Young's modulus of $E_{<0001>}$=150 GPa[10] and Poison's ratio of $\nu_{<0001>}$=0.38[17], the Raman shift implies an estimated stress of 0.502 GPa.

Figure 5 shows the room-temperature PL spectra of the InGaN/GaN LED samples with and without the inclusion of the GaN nanopattern. The LED sample without the nanopatterned bottom PC surface shows PL peaks at 373 and 443 nm, corresponding to the origins of GaN band-to-band edge transition and the quantum well exciton level, respectively. However, the nanopatterned bottom PC LED sample shows PL peaks at 431 and 506 nm. The broad yellow PL band at 582 nm comes from the influence of the threading dislocation[18].

The reference sample without a bottom PC has an In mole fraction of x=0.18 corresponding to a PL peak at 443 nm for a free-standing InGaN/GaN MQW LED layer. However, the bottom PC sample with the nanopattern has two In fractions of x=0.16 and 0.24 for the corresponding PL peaks at 431 and 506 nm, respectively, and it shows a relatively dominant intensity for the spectrum at 506 nm. The PL peak at 431 nm is similar to the free-standing zone of the reference sample. This indicates that an In mole fraction of x=0.18 in the flat surface of reference sample can be shifted into two phases of In mole fractions: x=0.16 and x=0.24 in the nanopatterned surface of the bottom PC sample. This phase separation can be correlated with the nanosurface tension and In segregation during the epitaxial growth on the nanopatterned surface of the bottom PC sample. The dominant PL intensity of the 506 nm shows the increased In mole fraction due to the enhanced solid solution on the nanopatterned surface. It is further desirable to search the electroluminescence spectra on the nanopatterned surface effect.

4. SUMMARY

In summary, the influence of the nanopatterned photonic

crystal effect on photoluminescence was demonstrated in an InGaN/GaN MQW LED structure deposited by MOCVD. The deposited GaN epitaxial surface has been nanopatterned with a hexagonal lattice of 230 nm. The regrown structure shows a Raman shift of transverse optical phonon mode to 569.5 cm^{-1}, which is similar to n-GaN thin films grown on a sapphire substrate. However, the regrown thin film without the nanopattern shows a free standing mode of 567.6 cm^{-1}. This result indicates that the nanohole surface plays the role of lattice-fixing points to preserve the strain energy for pseudo-morphic growth. The compressive strain in the nanopatterned GaN layer can be transferred into the regrown GaN layer, and the nanopattern provides a better environment for the lateral regrowth of the thin film. To conclude, a nanopatterned surface morphology can provide a good environment for epitaxial growth in spite of the built-in stress-strain effect from the sapphire substrate.

ACKNOWLEDGMENTS

This work was supported by the Korean Research Foundation Grant(KRF-2007-521-D00188).

REFERENCES

[1] S. Nakamura and G. Fasol, *The Blue Laser Diode: GaN Based Light Emitters and Lasers*, (Springer, Berlin, 1997) p. 203.

[2] G. S. Shin, S. W. Hwang, and K. Kim, Trans. Electr. Electron. Mater. **4,** 19 (2003).

[3] K. Kim, Trans. Electr. Electron. Mater. **5** 174 (2004).

[4] A. Sakai, H. Sunakawa, and A. Usui, Appl. Phys. Lett. **71,** 2259 (1997).

[5] T. S. Zheleva, O. H. Nam, M. D. Bremser, and R. F. Davis, Appl. Phys. Lett. **71,** 2472 (1997).

[6] D. S. Wuu, W. K. Wang, K. S. Wen, S. C. Huang, S. H. Lin, R. H. Horng, Y. S. Yu, and M. H. Pan, J. Electrochem. Soc. **153**, G765 (2006).

[7] T. V. Cuong, H. S. Cheong, H. G. Kim, H. Y. Kim, C.-H. Hong, E. K. Suh, H. K. Cho, and B. H. Kong, Appl. Phys. Lett. **90**, 131107 (2007).

[8] C. H. Chiu, H. H. Yen, C. L. Chao, Z. Y. Li, P. Yu, H. C. Kuo, T. C. Lu, S. C. Wang, K. M. Lau, and S. J. Cheng, Appl. Phys. Lett. **93**, 081108 (2008).

[9] J. Park, J.-K. Oh, K.-W. Kwon, Y.-H. Kim, S.-S. Jo, J. K. Lee, and S.-W. Ryu, IEEE Photonics Technol. Lett. **20**, 321 (2008).

[10] V. A. Savastenko and A. U. Sheleg, Phys. Status Solidi A, **48**, K135 (1978).

[11] D. C. Look and J. R. Sizelove, Phys. Rev. Lett. **82**, 1237 (1999).

[12] K. Kim and S. J. Chung, Trans. Electr. Electron. Mater. **2**, 24 (2001).

[13] M. Jamil, J. R. Grandusky, V. Jindal, F. Shahedipour-Sandvik, S. Guha, and M. Arif, Appl. Phys. Lett. **87**, 082103 (2005).

[14] L. S. Wang, K. Y. Zang, S. Tripathy, and S. J. Chua, Appl. Phys. Lett. **85**, 5881 (2004).

[15] T. S. Jeong, C. J. Youn, M. S. Han, J. W. Yang, and K. Y. Lim, Appl. Phys. Lett. **83**, 3483 (2003).

[16] H. Hartono, C. B. Soh, S. Y. Chow, S. J. Chua, and E. A. Fitzgerald, Appl. Phys. Lett. **90**, 171917 (2007).

[17] T. Detchprohm, K. Hiramatsu, K. Itoh, and I. Akasaki, Jpn. J. Appl. Phys. **31**, L1454 (1992).

[18] K. Kim and C. B. Park, Thin Solid Films, **330**, 139 (1998).